Gradually tapered hollow glass waveguides for the transmission of CO_2 laser radiation

Daniel J. Gibson and James A. Harrington

Hollow glass waveguides with bores tapered from 1000 to 500 μm and from 700 to 500 μm over a length of 2 m were coated with silver and silver iodide inner films. These waveguides were designed for low attenuation at the 10.6-μm CO_2 laser wavelength. The straight losses, which were measured to be 0.8 and 1.6 dB/m, respectively, decreased when the guides were bent. A simple ray-trajectory model is presented to explain this unexpected behavior. © 2004 Optical Society of America

OCIS code: 060.2390.

1. Introduction

Leaky-type, hollow glass waveguides (HGWs) have proven to be an excellent IR fiber optic for the delivery of IR laser power.[1,2] This type of waveguide typically consists of a reflective (metallic) layer and a reflection-enhancing (dielectric) layer deposited on the inside of a hollow substrate. A typical HGW generally employs a silver film and a single-dielectric layer of either a metal halide, such as AgI,[3] or a polymer,[4] such as cyclic olefin, deposited on the inside surface of small-bore silica tubing, as shown in Fig. 1. These waveguides have very low loss and high spatial purity of the output beam profile as a result of the smooth inner surface of the glass substrate tubing.

The attenuation coefficient, α, in a constant-bore HGW is dependent on many factors, including wavelength, bore size, and bending radius. There are many excellent reviews[1,2] of HGWs, but in general the straight loss, α_∞, for the leaky-type waveguide shown in Fig. 1 is given by

$$\alpha_\infty = \left(\frac{u_m}{2\pi}\right)^2 \frac{\lambda^2}{a^3} \left(\frac{n}{n^2 + k^2}\right)_{\text{metal}} F_{\text{film}}, \qquad (1)$$

where u_m is the mode parameter, a is the bore radius, λ is the wavelength, n and k are the optical constants of the metal film, and F_{film} is a loss term for the dielectric coating(s).[5] In addition, there is a loss on bending for these single-dielectric HGWs that varies as $1/R$, where R is the radius of bending.[6] We note from Eq. (1) that the losses increase rapidly as the bore size decreases and that the loss increases for higher-order modes. The lowest loss is for the lowest-order HE_{11} mode, i.e., when $u_m = 2.405$.

Tapered-bore hollow glass waveguides can be divided into two types: short (or fast) and long (or gradual) tapers. Short tapers are tapered at a steep angle ($\geq 1°$) over a short distance, typically 3–10 cm, and are used in conjunction with nontapered HGWs at the input or proximal end to reduce coupling losses (tapered couplers)[7–9] or at the output or distal end to reduce spot size and to increase power density (tapered tips).

Long, gradually tapered HGWs, which are the focus of this study, are tapered at a very small angle ($<0.1°$) and are intended to be used in place of traditional, nontapered guides. The large bore at the proximal end improves coupling, and the small bore at the distal end allows for the enhanced flexibility required in a variety of applications, including minimally invasive surgical and diagnostic procedures.

2. Experiment

Metallic silver and dielectric silver iodide films, optimized for low loss at 10.6 μm, were deposited on the inside of tapered silica tubing by use of a liquid phase reaction technique.[10] To ensure consistent wetting of the capillary walls, coating solutions were introduced into the large bore end of the tapered tubing. The silica glass tubing was drawn from a hollow preform by FiberGuide Industries of Stirling, N.J. A linear taper was achieved by varying the capstan speed relative to the preform feed rate. Two sizes of

The authors are with the Department of Ceramic and Materials Science and Engineering, Rutgers University, 607 Taylor Road, Piscataway, New Jersey 08854. J. Harrington's e-mail address is jaharrin@rci.rutgers.edu.

Received 24 September 2003; revised manuscript received 8 January 2004; accepted 12 January 2004.

0003-6935/04/112231-05$15.00/0

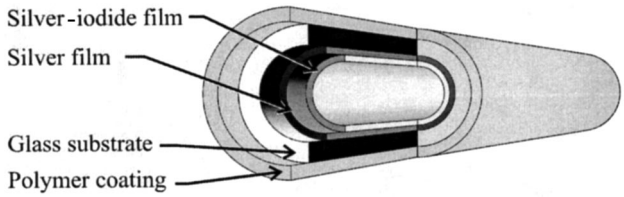

Fig. 1. Cutaway of a typical HGW structure revealing metallic (silver) and dielectric (silver iodide) layers.

taper were fabricated with bores tapered from 1000 to 500 μm over a length of 2 m and from 700 to 500 μm over 2 m.

The spectral response of the tapered waveguides was measured with Fourier-transform IR spectroscopy. The spectra obtained from short, 10-cm-long waveguide pieces taken from either end of the tapered guide showed a slight shift in the interference peaks, which indicates that the dielectric silver iodide film thickness is ~5% thinner at the small bore end. However, this thickness change is comparable with that routinely observed for nontapered HGWs of similar length and with the same fabrication protocol.[11]

3. Measurements

Straight losses were measured with a 20-W linearly polarized, actively stabilized, sealed cavity CO_2 laser (MPB Communications, Inc., GN-series). Various ZnSe lenses were used to attain maximum coupling and minimal loss. These straight losses, summarized in Table 1, were consistently higher than those of similarly sized nontapered HGWs. The bending loss for tapered hollow waveguides was investigated by bending the individual guides to a constant curvature at various radii between 0.5 and 3 m. Contrary to the trend observed for nontapered waveguides, the loss for tapered waveguides decreased with bending. Bending losses for the tapered guides, along with the bending loss behavior for a 700-μm constant-bore waveguide, are shown in Fig. 2. At 20-W cw incident power, the maximum curvature attained before the tapered waveguides failed near the small bore end was 2 m^{-1}.

4. Discussion

The observed straight and bending loss behavior of tapered hollow waveguides may be explained in terms of the generation of higher-order modes as light propagates through the waveguide. The fractional coupling coefficient, η_m, for a given hybrid mode is

$$\eta_m \cong \frac{(m - 1/4)\lambda^2}{\theta_0^2 a^2} \exp\left[-\frac{(m - 1/4)^2\lambda^2}{2\theta_0^2 a^2}\right], \quad (2)$$

where θ_0 is the coupling angle and m is the mode index.[12] This implies that, in a tapered waveguide, as the HE_{11} mode propagates and its coupling angle increases, some of its power is transferred to higher-order modes. Therefore the waveguide loss given in Eq. (1) increases as the number of propagating modes increases. That is, the propagation of higher-order modes with large mode parameters u_m greatly increases α_∞.

This can also be seen from an examination of the ray-angle trajectory for a distribution of launch angles representing a focused Gaussian beam and accounting for power loss for each reflection at the waveguide wall. Zhou *et al.*[13] used a similar ray-trajectory analysis to evaluate the transmission loss of a long, nontapered hollow waveguide with and without a short tapered coupler at the input end. They found that when the focused spot size was greater than 63% of the waveguide bore, the total transmission loss was reduced when a tapered coupler was used. Our ray-trajectory analysis uses an iterative approach similar to that used by Zhou *et al.* for short tapered couplers, but predicts the transmission losses for both straight and bent gradually tapered, long hollow waveguides.

First, for a straight tapered guide with a given launch angle, θ_0, the initial angle of incidence, ψ_0, at the start of the traverse ($z = 0$) is

$$\psi_0 = \pi/2 - \theta_0 - \delta\psi/2, \quad (3)$$

where $\delta\psi$ is the angle of the taper

$$\delta\psi = 2 \tan^{-1}\left(\frac{a_1 - a_2}{2L}\right) \quad (4)$$

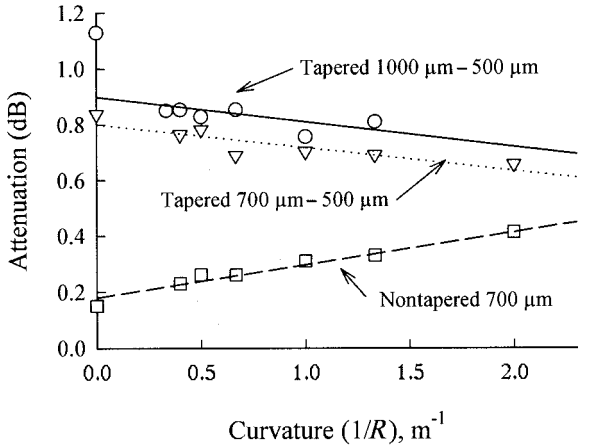

Fig. 2. Measured bending losses of tapered (1000–500 μm and 700–500 μm) and continuous bore (700 μm) HGWs at 10.6 μm.

Table 1. Tapered and Nontapered HGW CO_2 Laser Losses

HGW Type	Bore Size (μm)	Attenuation (dB/m)
Tapered	1000–500/2 m	0.80
	700–500/2 m	0.40
Nontapered	1000	0.10
	700	0.13
	530	0.22

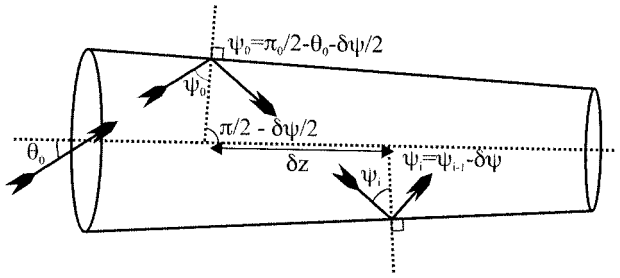

Fig. 3. Ray-trajectory model for transmission of a linearly tapered, unbent hollow waveguide.

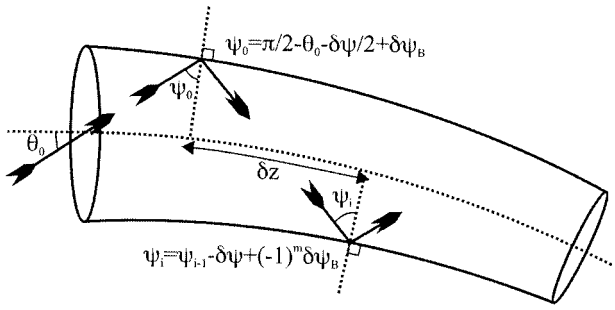

Fig. 4. Trajectory model for a bent tapered waveguide, based on the SWA, is valid for large bending radii.

for a waveguide tapered from a_1 to a_2 over a length L. This ray trajectory is shown in Fig. 3. For successive bounces, the angle of incidence decreases by $\delta\psi$

$$\psi \rightarrow \psi - \delta\psi, \tag{5}$$

the power decreases proportional to the wall reflectivity

$$P_\theta \rightarrow P_\theta R(\psi), \tag{6}$$

and the axial distance δz is traversed

$$\begin{aligned} z &\rightarrow z + \delta z \\ &\rightarrow z + a(z)\tan(\psi), \end{aligned} \tag{7}$$

where $a(z)$ is the bore profile of the tapered waveguide

$$a(z) = a_1 - z\,\frac{a_1 - a_2}{L}. \tag{8}$$

The first few rays are shown in Fig. 3, and this process is repeated until the ray either exits the waveguide or turns around and is effectively lost. Integrating the transmitted power, P_θ, over the incident beam profile, $I(\theta)$, gives the transmission loss for the tapered waveguide:

$$\alpha = -\frac{10}{L}\log\left[\frac{\int_0^{\theta_{\max}} I(\theta)P_\theta(\theta)\sin\theta\,d\theta}{\int_0^{\theta_{\max}} I(\theta)\sin\theta\,d\theta}\right]. \tag{9}$$

When the tapered waveguide is bent to large radii, as shown in Fig. 4, the straight waveguide model is modified to accommodate the change in propagation angle due to bending:

$$\delta\psi_B \cong \frac{a(z)}{R}\tan\psi. \tag{10}$$

The incident angle decreases by $\delta\psi_B$ for bounces along the outer wall and increases by $\delta\psi_B$ for bounces along the inner wall. Equation (5) then becomes

$$\psi \rightarrow \psi + (-1)^k\,\frac{a(z)}{R}\tan\psi \tag{11}$$

for the kth bounce. This straight waveguide approximation (SWA) is valid only for large bending radii.

When the bending radii are small, ray propagation in a curved tapered (or nontapered) waveguide follows the edge-guided mode (EGM), also called the whispering gallery mode, as shown in Fig. 5. In this method of propagation, the guided ray follows the outer waveguide wall only, and the incident angle is invariant:

$$\psi_i = \psi_0 = \pi/2 - \theta_0 - \delta\psi/2. \tag{12}$$

The traversed distance is also constant in the EGM:

$$\begin{aligned} \delta z &= (\pi - 2\psi_i)R \\ &= (2\theta_0 + \delta\psi)R. \end{aligned} \tag{13}$$

Compared with SWA trajectories, EGM trajectories yield a lower attenuation because the incident angle is relatively small and constant and the number of bounces is much smaller.

For a given distribution and tapered waveguide geometry, some rays follow wholly EGM or SWA trajectories, whereas others begin in the EGM and transition to the SWA as the waveguide bore becomes small. In particular, the EGM–SWA transition oc-

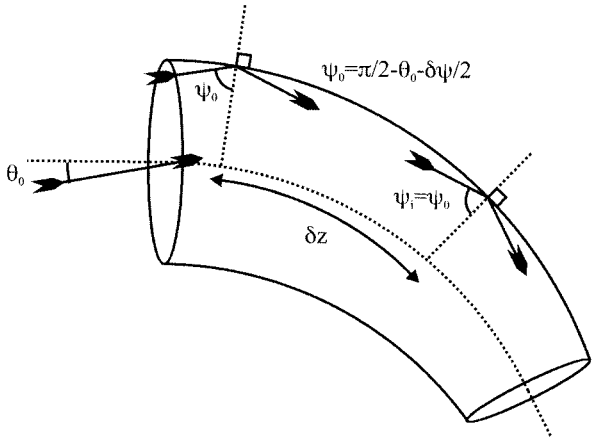

Fig. 5. Edge-guided trajectory (whispering gallery mode) is applicable when tapered (or nontapered) hollow waveguides are bent to small radii.

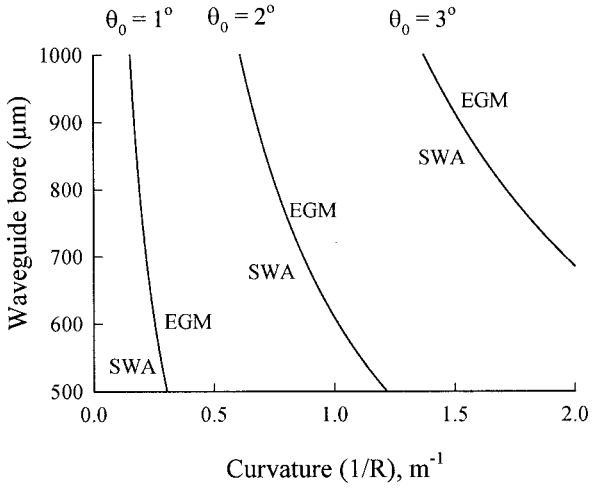

Fig. 6. Critical waveguide bore for transition between the EGM and the SWA bending loss trajectories.

curs when the waveguide bore is less than the critical bore size:

$$a_c = R\left[1 - \cos\left(\frac{\pi}{2} - \psi\right)\right]. \tag{14}$$

The critical bore size for the EGM–SWA transition is shown graphically in Fig. 6 for various launch angles.

The bending losses for the tapered and nontapered waveguides used in this study were calculated with the EGM–SWA hybrid model and are shown in Fig. 7 for a 2° focused Gaussian beam. These curves reveal local maxima for large bending radii ($1/R \sim 0.25$ m^{-1}), indicating the dominance of the high-loss SWA mode of propagation. The loss then decreases with decreasing bending radius, and more rays follow EGM trajectories. As the waveguides are bent to even smaller radii ($1/R > 2$ m^{-1}), attenuation increases approximately linearly as the lower-loss

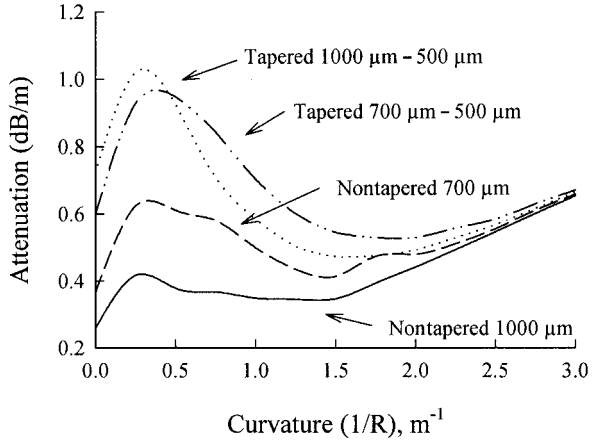

Fig. 7. Bending losses for tapered- and continuous-bore HGWs with inner silver and silver iodide films as predicted by the combined EGM–SWA trajectory model with a 2° divergent focused Gaussian beam at 10.6 μm.

EGM propagation mode becomes dominant. In this region, waveguide loss is directly proportional to the curvature, 1/R. Although the waveguide losses measured and shown in Fig. 2 do not agree exactly with those calculated by this model, they do follow the general predicted trend.

The main flaw in this model is that it considers only trajectories that lie entirely within the plane of bending. Trajectories outside plane components make up a significant portion of the delivered light and should not be ignored. Such trajectories are more complicated than those presented here, and thus the present method does not apply to them. The current model does however give insight into the slightly decreased bending loss exhibited by the tapered waveguides.

5. Conclusions

Tapered HGWs were fabricated and shown to exhibit losses higher than those observed in similarly sized nontapered guides. Although the measured absorption coefficients of the tapered waveguides in this study were high, the attenuation decreased with bending. This phenomenon was explained by means of a simplified ray-trajectory model that considered propagation via the SWA, the EGM (whispering gallery mode), as well as the transitions from EGM to SWA.

A common disadvantage of using HGWs in power-delivery applications is the fluctuation in output power due to arbitrary bending geometry and large bending losses. In this paper we have shown that this effect can be reduced in practice through the use of a tapered waveguide, the attenuation coefficients of which are less sensitive to bending. The guides in this paper were capable of delivering 15 W of CO_2 laser power at the distal end.

References

1. J. A. Harrington, "Infrared fiber optics," in *Handbook of Optics*, Vol. III, M. Bass, J. Enoch, E. Van Stryland, and W. Wolfe, eds. (McGraw-Hill, New York, 2001).
2. J. Harrington, "A review of IR transmitting, hollow waveguides," Fiber Integr. Opt. **19,** 211–227 (2000).
3. K. Matsuura, Y. Matsuura, and J. A. Harrington, "Evaluation of gold, silver, and dielectric-coated hollow glass waveguides," Opt. Eng. **35,** 3418–3421 (1996).
4. Y. Abe, Y. Matsuura, Y. W. Shi, Y. Wang, H. Uyama, and M. Miyagi, "Polymer-coated hollow fiber for CO_2 laser delivery," Opt. Lett. **23,** 89–90 (1998).
5. M. Miyagi and S. Kawakami, "Design theory of dielectric-coated circular metallic waveguides for infrared transmission," IEEE J. Light. Technol. **LT-2,** 116–126 (1984).
6. M. Miyagi, K. Harada, and S. Kawakami, "Wave propagation and attenuation in the general class of circular hollow waveguides with uniform curvature," IEEE Trans. Microwave Theory Tech. **MTT-32,** 513–521 (1984).
7. Y. Matsuura, H. Hiraga, W. You, Y. Kato, M. Miyagi, S. Abe, and S. Onodera, "Lensed-taper launching coupler for small-bore, infrared hollow fibers," Appl. Opt. **36,** 7818–7821 (1997).
8. H. Hiraga, Y. Matsuura, M. Miyagi, S. Abe, S. Onodera, and J. A. Harrington, "Design and transmission characteristics of lensed-taper launching coupler for infrared hollow fibers," Rev. Laser Eng. **26,** 331–334 (1998).

9. K. Iwai, Y. Abe, Y. Matsuura, and M. Miyagi, "Equivalent complex refractive indices for ray-tracing evaluation of dielectric-coated hollow waveguides," Opt. Eng. **41,** 1471–1472 (2002).
10. C. D. Rabii, D. E. Dobin, D. J. Gibson, and J. A. Harrington, "Recent advances in the fabrication of hollow glass waveguides," in *Surgical Assist Systems*, M. S. Bogner, S. T. Charles, W. S. Grundfest, J. A. Harrington, A. Katzir, L. S. Lome, M. W. Vannier, and R. von Hanwehr, eds., Proc. SPIE **3262,** 125–129 (1998).
11. C. Rabii and J. A. Harrington, "Measurement and control of thin film uniformity on hollow glass waveguides," Opt. Eng. **38,** 2009–2015 (1999).
12. M. Saito, S. Sato, and M. Miyagi, "Loss characteristics of infrared hollow waveguides in multimode transmission," J. Opt. Soc. Am. A **10,** 277–282 (1993).
13. J. Y. Zhou, Y. J. Deng, N. Ling, G. N. Lu, and Z. X. Li, "Laser transmission through a dielectric-coated hollow tapered metallic waveguide," Opt. Commun. **142,** 30–33 (1997).